

DRA-4. MINERALOGICAL CHARACTERIZATION OF QUESTA ROCK-PILE SAMPLES BY PETROGRAPHIC AND ELECTRON MICROPROBE ANALYSIS

N. Dunbar, L. Heizler, D. Sweeney, May 21, 2007, revised November 6, 2008 (reviewed by V.T. McLemore)

1. STATEMENT OF THE PROBLEM

What is the current mineralogy and mineral chemistry of the Questa rock piles? How has the mineralogy and mineral chemistry of the components of the Questa piles changed since deposition 25-40 years ago? What are the textures and relationships between minerals in the rock piles?

2. PREVIOUS WORK

The work presented here builds on ongoing research on the Questa rock piles. Some of those results are included in the following papers: Dunbar et al., (2005), McLemore et al. (2006a, b, 2008a), and Phillips et al. (2005). In addition to the focused studies listed above, a number of relevant studies have addressed the geological history, mineralogy, geochemistry, and alteration history of the volcanic and plutonic rocks of the Questa region (summarized by McLemore, 2008a). These are included in the reference list.

3. TECHNICAL APPROACH

The technical approach to this component has involved a combination of petrography (described in SOP 24) and electron microprobe analyses on rock samples to determine the mineral phases present, mineral chemistry and to examine textural relationships between mineral phases (described in SOP 26).

Several different types of samples were collected (DRA 0):

- Samples of the rock pile material (5 ft channel or selected layers)
- Soil profiles of colluvium/weathered bedrock, alteration scar, and debris flows
- Outcrop samples of unweathered (or least weathered) igneous rocks representative of the overburden
- Drill core samples of the overburden and ore deposit before mining
- Drill cuttings from holes drilled into the rock piles and underlying colluvium/bedrock
- Samples selected for specific analysis (age dating, stable isotopes, etc)

Details of sample collection and analysis are in the project SOPs and summarized in DRA 0. The collected samples from the rock piles consisted of a heterogeneous mixture of rock fragments ranging in size from boulders (0.5 m) to <1 mm in diameter within a fine-grained soil matrix. Most rock fragments are hydrothermally altered before mining occurred; some are oxidized and weathered since emplacement in the rock pile. During the probe analysis, both rock fragments and soil matrix of each sample were examined. Field photos of each sample are in McLemore et al. (2008a, b), other project reports, and the project data repository.

4. CONCEPTUAL MODEL

Our conceptual model is that Questa rock piles were formed of variably hydrothermally altered igneous rocks that have undergone some changes in mineralogy since the time of

their emplacement into the rock pile. The two main rock types seen in the rock piles are andesitic lava and rhyolitic ignimbrite (Amalia Tuff), and these rocks appear to have undergone quartz-sericite-pyrite (QSP), and/or propylitic-argillic alteration prior to rock pile deposition. No detectable changes in the silicate minerals appear to have taken place since the time of deposition in the rock piles. However, we do observe evidence for dissolution of pyrite and carbonate, as well as the formation of gypsum, Fe oxide (goethite, hematite), and jarosite, subsequent to deposition of the rock pile. These phases may provide cementation of the matrix material in the rock pile, particularly on the outer rock pile surfaces.

5. STATUS OF COMPONENT INVESTIGATION

PETROGRAPHIC RESULTS

Soil petrography was determined using predominantly examination of a split of the rock pile material using a binocular microscope. Selected thin sections of the rock-pile material and rock samples were examined using a petrographic microscope. Three rock types are observed in the Goathill North (GHN) rock pile material: andesite, rhyolitic ignimbrite (Amalia Tuff) and igneous intrusions (granite, aplite). Figure 1a shows the variation in lithology with respect to geological units identified within the rock pile. The units are shown in progression from the outermost portion of the rock pile (Unit I) towards the inner most portions (Unit M). Andesite is the predominant lithology overall. Noted exceptions are Units J and M, in which Amalia Tuff dominates. Intrusive rocks, although present within colluvium/weathered bedrock, alteration scar, debris flows and other rock piles, are minor to absent within the GHN rock pile. However, the range in rock types for individual units is large, in most cases, covering the entire range of variability between all of the different units.

A wide range of minerals are observed petrographically in the studied samples. The main phases present include quartz, potassium feldspar, plagioclase, epidote, pyrite, authigenic gypsum, detrital gypsum, jarosite and several clay minerals, including illite and chlorite. The relative abundance of these phases is estimated using other techniques (see DRA-5) and will not be discussed here.

As mentioned above, many of the rocks found in the GHN rock pile have undergone hydrothermal alteration. Three types of alteration have been described, including propylitic, quartz-sericite-pyrite (QSP), and argillic (McLemore et al., 2008b). Rough estimates of the intensity of these three alteration styles in the GHN rock pile were made petrographically (Fig. 1b). Although the ranges of intensity of alterations styles within a single rock pile unit are large, some observations can be made. First, QSP alteration is the most prevalent style, and argillic alteration is relatively minor. Propylitic alteration is present throughout the pile, although, on average, at a lower intensity than QSP. There appears to be slightly more propylitic alteration in the interior rock pile units.

Examples of photos taken during petrographic characterization are shown in Figure 2; additional photos are in the project data repository. Authigenic gypsum is often found in the presence of detrital gypsum (Fig 2a). Detrital gypsum is recognized by its milky color and blocky shape, whereas authigenic gypsum forms clear, platy or fuzzy crystals (Campbell and Lueth, 2008). The crystals often exhibit the indicative crystal

habit of gypsum. Although pristine pyrite is the norm, goethite often replaces pyrite (Fig. 2b) and tarnished (oxidized) pyrite grains (Fig. 2c) have been noted in several samples.

ELECTRON MICROPROBE RESULTS

Igneous mineralogy and hydrothermal alteration phases

Electron microprobe observations are consistent with the petrographic observations indicating that two main rock types, andesitic lava and rhyolitic ignimbrite, are present in the rock pile samples. Typical mineral phases observed in both rock fragments and fine-grained matrix include feldspar, quartz, pyrite, chlorite, epidote, clay minerals, gypsum, carbonate, Fe oxide phases, rutile, zircon, and alteration products of pyrite (see selected compositions in Table 1, Appendix 1). The mineral jarosite is generally not observed in samples from the interior of rock piles, but is abundant in samples taken from the outer rock pile surface, as well as in samples taken from beneath the rock pile (i.e. colluvium and weathered bedrock, McLemore, 2008b).

The electron microprobe analyses of rock-pile samples show evidence of propylitic and QSP hydrothermal alteration, although relict igneous textures are typically evident. Most samples contain clay minerals and both chloritic and illitic/sericitic compositions are common. Feldspar compositions are generally alkaline, and show evidence of alteration from original igneous composition. This alteration is thought to be a result of hydrothermal alteration of the original igneous feldspar composition. Feldspars contain abundant clay-rich pockets, and the clay compositions are consistent with formation by hydrothermal processes. The feldspar crystals do not show any evidence of dissolution or chemical leaching, which could be inferred if the edges of the feldspar crystals were ragged or if there was evidence of chemical variability associated with the crystal edges or along fractures. Epidote is present in many samples, and carbonate is observed in some. Both appear to be a result of hydrothermal alteration of the original igneous rock.

In addition to rock fragments, the matrix or soil, component of a number of samples was also investigated. The soil samples are composed of small mineral or rock fragments in a clay-rich matrix (Fig. 3). Typically, the mineralogy of the small mineral and rock fragments in the soil is similar to the larger rock fragments from the same sample. However, the soil component tends to be much more clay-rich. The clay compositions are similar to those observed in the rock fragments (Table 2, see also DRA 3 on clay mineralogy). This clay may be a result of breaking of rock fragments and resultant removal of clay from within the rock.

Pyrite

Pyrite is observed in many samples, pristine in some cases, altered in others. The genesis and timing of pyrite alteration, as well as distribution of altered pyrite within rock piles, is uncertain, but likely a result of two more stages of hydrothermal alteration (Molling, 1989; McLemore et al., 2008a). Unaltered pyrite typically occurs as well-crystallized cubes or groups of cubes and is found as inclusions within rock fragments as well as in the matrix material between rock fragments (Fig. 4 and 5). Pyrite exhibits a range of alteration styles. Some pyrite grains display oxidized rims, suggesting alteration that is proceeding from the outside inward (Fig. 6). In other samples, void areas around pyrite grains suggest that alteration has taken place, but that the resultant alteration material has

been completely removed (Fig. 7). Some pyrite grains in soil samples appear almost completely oxidized, and due to their skeletal appearance, oxidation appears to have taken place in situ (Fig. 8). The unlikelihood that these delicate forms would have survived transport and deposition in the rock pile is the strongest evidence we have observed that pyrite oxidation occurred following rock pile deposition.

Detailed electron microprobe observations indicate that even very thin “tarnishing” of pyrite grains can be observed using BSE imaging. The chemical composition of oxidized rims on pyrite has also been investigated, and suggests that during the oxidation process, S is lost from the pyrite, but that the resulting Fe oxide (goethite, hematite) may contain significant Si, Al, and P (see details in Fe oxide section below).

Fe oxide (goethite, hematite)

A Fe-rich phase is observed in many samples of rock pile and scar material. Definitive identification of this phase using the electron microprobe is problematic because analytical totals are consistently low, suggesting the presence of elements that we cannot directly analyze, particularly O and H. However, based on the association of this phase, as well as the chemical composition based on the elements that we are able to analyze, we postulate that this phase consists largely of the mineral goethite (which is a Fe oxyhydroxide). The reflectance spectroscopy analysis indicates that goethite is more prevalent than hematite, although both are present (project database, Phoebe Hauff, written communication, 7/7/04).

The goethite in these samples occurs in a number of forms. First, we observed goethite directly associated with pyrite grains, probably as the result of pyrite oxidation (Figs. 6 and 8). Goethite also occurs as complete replacement of grains that were probably originally pyrite, but in which the pyrite has been completely altered (Fig. 9). Goethite also occurs as fracture filling (Fig. 10), as coatings on rock fragments (Fig. 11).

Goethite found in rock pile samples may have multiple origins. The delicate goethite that is found replacing pyrite grains is likely to be formed in the rock pile because it would be difficult for such delicate structures to survive transport. In some rock fragments, goethite is more abundant near the margin of the rock fragment than in the core. This also argues for formation in the rock pile. The same argument can be made for goethite that is found as a coating on rock fragments. However, loose fragments of goethite in the matrix, fracture-filling goethite, and massive goethite replacing pyrite may be inherited from the hydrothermally altered source rocks. A notable aspect of the goethite in the rock pile and scar samples is that the chemical compositions are variable. As would be expected, most goethite contains Si in addition to Fe and Al is also typically observed (Appendix 1). A subset of the goethites also contain P and S (Appendix A). The abundance of the oxides of Si, Al, P and S can be as high as 10 wt.%. There does not appear to be any systematic correlations between the 4 elements, but this has not been investigated in detail. As can be seen in Fig. 9, many goethites appear banded in BSE imaging, suggesting compositional variability over a short distance.

Jarosite

Jarosite is common in soil samples from the outer parts of rock piles. Several morphologies of jarosite are observed, all of which are interpreted to be authigenic.

Jarosite is commonly present in irregular patchy areas, typically with rounded edges, in the matrix of soil samples (Fig. 12). These patchy areas often occur in association with goethite. These isolated patches may not substantially affect cementing or sample cohesion. The patches shown in Figure 12 consist of very fine masses of jarosite granules. In some samples, granular jarosite forms within the soil matrix and also fills fractures within altered rock fragments, in which case the jarosite may contribute substantially to cohesion (Fig. 13). Jarosite also occurs as a replacement phase within relict pyrite cubes (Fig. 14).

Tiny distinct euhedral crystals of jarosite are occasionally present in the soil matrix (Fig 15), but more commonly jarosite is finely intermixed with clay. Intermixed jarosite is thought to contribute to overall sample cohesion. Jarosite is sometimes observed as localized patches of cement intergrown within the soil matrix (Fig. 16) or as vein filling within altered rock fragments, often in association with goethite. Both morphologies appear to add to sample cohesion. In some samples, jarosite occurs in association with gypsum. Figure 18 shows delicate gypsum rosettes within jarosite cement, and in Figure 19, a jarosite vein occurs in association with finely intergrown gypsum.

Gypsum

Gypsum is common in soil samples from the rock piles. Two primary morphologies of gypsum are observed, one consisting of large single gypsum crystals (Fig. 17; Dunbar et al., 2005) and the other of very small, dominantly aggregate blades. Some large grains appear eroded and are interpreted to be detrital (i.e., part of the original depositional rock pile material; Campbell and Lueth, 2008). Other grains, despite partial to complete plucking during sample preparation, appear fairly well preserved or leave well preserved euhedral casts, suggesting that at least some of these larger crystals may be authigenic (formed in the rock piles since deposition).

Demonstrably authigenic gypsum is also present in the form of very fine blades or rosettes typically observed around the margins of clots of soil material. The well-preserved nature of these delicate forms suggests that they formed in situ (Fig. 18). In some samples, delicate gypsum needles, some interconnected, are found throughout the clay matrix of altered rock fragments (Fig. 19) and within soil matrix. This level of gypsum abundance is typically observed in samples from the outer part of the rock pile and may contribute to the cohesiveness of the rock pile matrix material.

6. RELIABILITY ANALYSIS

Assumptions/Limitations of Petrographic Characterizations

The primary limitation of the data lies in the estimation of mineral abundances, lithology abundances and alteration intensity. The American Geological Institute (AGI) provides the comparison charts that we use to estimate volume abundance of minerals and lithologies. This estimation may vary slightly from user to user; hence the dataset is only semi-quantitative. Moreover, there is no set protocol to determine alteration intensity, thus this data may vary widely between different petrographers. Like the electron microprobe analysis, the petrography data is collected on a relatively small sample, i.e. hand-sample sized to fine-grained sand sized particles. We recognize that the data

obtained from these analyses may not be completely representative. However, we assume the interpretations may be applied to the larger scale rock pile.

Assumptions/Limitations of Electron Microprobe Analysis

The principal limitation of the electron microprobe data is that the samples analyzed are very small, and therefore cannot fully represent the entire spectrum of mineral compositions, morphologies and textures present within a given rock pile unit. The assumption made as part of microprobe analysis is that, although our samples are small, the interpretations made from our analyses are relevant, and provide insight into processes occurring in the rock piles.

7. CONCLUSIONS OF THE COMPONENT

- The GHN rock pile is constructed of hydrothermally altered igneous rock. The two principal rock types are rhyolitic ignimbrite, likely Amalia Tuff, and andesitic lava. Two predominant types of hydrothermal alteration, quartz-sericite-pyrite (QPS) and propylitic-argillic, are recognized.
- No definitive evidence of major weathering of feldspar component of the rocks is observed, either related to formation of new clay minerals from feldspar, or by dissolution or leaching of feldspar. The clay minerals in the rock fragments and loose soil matrix appear very similar, suggesting that no formation of new clay minerals is taking place. However, small-scale leaching of clay minerals in the soil matrix or rock fragments, or small-scale leaching or dissolution of feldspar, cannot be ruled out based on our observations.
- In the time since rock pile deposition, a number of mineralogical changes have demonstrably occurred. These include alteration of pyrite and dissolution of carbonate, as well as in-situ formation of gypsum and jarosite. The latter two phases may provide cementation of the matrix, or soil, component of the rock pile.
- The mineral goethite is inferred to be present in many rock pile samples. Some of this goethite is probably inherited from the source rocks, but some, particularly where replacing pyrite, it thought to be forming in the rock pile during weathering. The observed goethite exhibits striking chemical variability, and can contain up to 10 wt% of SiO₂, Al₂O₃, P₂O₅ or SO₂.
- The abundance of secondary jarosite is strongly linked to location within the rock pile. Jarosite is found in samples from the outer parts of, as well as beneath the GHN rock pile.
- Qualitative electron microprobe observations suggest that gypsum is also more abundant in samples from the outer parts of the GHN rock pile. This is not observed petrographically, possibly because much of the authigenic gypsum is too fine to be observed using the petrographic techniques.
- The petrographic and electron microprobe work to date has provided general answers to the questions addressed in this component of the research. Ongoing analyses of rock pile and related material are anticipated to provide information that will allow our questions to be answered in greater depth.

8. REFERENCES

- Campbell, A.R. and Lueth, V.W., 2008, Isotopic and textural discrimination between hypogene, ancient supergene, and modern sulfates at the Questa mine, New Mexico: *Applied Geochemistry*, v. 23, no. 2, p. 308- 319.
- Dunbar, N., McLemore, V.T., Donahue, K., Heizler, L., Lueth, V.W., Phillips, E., 2005, Geochemistry, mineralogy, and electron microprobe investigation of the Goathill North Rock Piles: unpublished report to Molycorp, Inc., Task 1.4.2, 1.4.3.
- McLemore, V.T., 2008a, Geologic Setting and Mining History of the Questa mine, Taos County, New Mexico: Unpublished report to Molycorp, Inc, Task 1.2.2, B1.1, 27 p. (revised from appendix 1.1, May 2005 report).
- McLemore, V.T., 2008b, Characterization of weathered bedrock profile from Goathill North area, Questa mine, New Mexico: unpublished report to Chevron, Task B1.4.
- McLemore, V.T., Donahue, K., and Sweeney, D., 2008b, Lithologic atlas: revised unpublished report to Molycorp (revised from appendix 2.3, May 2005 report).
- McLemore, V.T., Donahue, K.M., Phillips, E.H., Dunbar, N., Walsh, P., Guitierrez, L.A.F., Tachie-Menson, S., Shannon, H.R., Lueth, V.W., Campbell, A.R., Wilson, G.W., and Walker, B.M., 2006a, Characterization of Goathill North mine rock pile, Questa molybdenum mine, Questa, New Mexico; in 7th ICARD, March 26-30, 2006, St. Louis MO.: Published by American Society of Mining and Reclamation., Lexington, KY. CD-ROM, p. 1219-1249.
- McLemore, V.T., Donahue, K., Phillips, E., Dunbar, N., Smith, M., Tachie-Menson, S., Viterbo, V., Lueth, V.W., Campbell, A.R., and Walker, B.M., 2006b, Petrographic, mineralogical and chemical characterization of Goathill North Mine Rock Pile, Questa Molybdenum Mine, Questa, New Mexico: 2006 Billings Land Reclamation Symposium, June, 2006, Billings, Mt. Published by Published by American Society of Mining and Reclamation, 3134 Montavesta Rd., Lexington, KY, CD-ROM.
<http://geoinfo.nmt.edu/staff/mclemore/Molycorppapers.htm>
- McLemore, V.T., Dickens, A., Boakye, K., Campbell, A., Donahue, K., Dunbar, N., Gutierrez, L., Heizler, L., Lynn, R., Lueth, V., Osantowski, E., Phillips, E., Shannon, H., Smith, M., Tachie-Menson, S., van Dam, R., Viterbo, V.C., Walsh, P., and Wilson, G.W., 2008a, Characterization of Goathill North Rock Pile: revised unpublished report to Molycorp, Tasks: 1.3.3, 1.3.4, 1.4.2, 1.4.3, 1.11.1.3, 1.11.1.4, 1.11.2.3, B1.1.1, B1.3.2.
- Molling, P. A., 1989, Applications of the reaction progress variable to hydrothermal alteration associated with the deposition of the Questa molybdenite deposit, NM: PhD dissertation, Johns Hopkins University, 227 p.
- Phillips, E.H., Lueth, V., Campbell, A., McLemore, V., Walker, B., and Tachie-Menson, S., 2005, Soil petrography of a sample traverse from a rock pile trench at the Questa Mine, New Mexico (abstr.): *New Mexico Geology*, v. 27, p. 47.

9. TECHNICAL APPENDICES

- Dunbar, N., McLemore, V.T., Donahue, K., Heizler, L., Lueth, V.W., Phillips, E., 2005, Geochemistry, mineralogy, and electron microprobe investigation of the Goathill North Rock Piles: unpublished report to Molycorp, Inc., Task 1.4.2, 1.4.3.

APPENDIX 1.

Table 1. Representative mineral compositions as analysed by electron microprobe

| FELDSPAR | SiO2 | Al2O3 | CaO | FeO | SrO | BaO | Na2O | K2O | Total | | | | | |
|-----------------------------|-----------------|------------------|----------------|----------------|----------------|----------------|----------------|----------------|--------------|--------------|------------|--------------|-----------|--------------|
| Potassic | | | | | | | | | | | | | | |
| Andesite ghn-nwd-0002-14 | 64.26 | 19.49 | 0.06 | 0.13 | 0.07 | 0.52 | 2.89 | 12.27 | 99.69 | | | | | |
| Andesite ghn-nwd-0021-20 | 64.12 | 19.18 | 0.00 | 0.00 | 0.00 | 0.04 | 0.47 | 16.77 | 100.57 | | | | | |
| Rhyolite ghn-kmd-0051-31-01 | 64.61 | 18.78 | 0.03 | 0.05 | 0.07 | 0.09 | 0.26 | 16.38 | 100.27 | | | | | |
| Rhyolite ghn-nwd-0023-03 | 63.37 | 18.76 | 0.02 | 0.00 | 0.00 | 0.13 | 0.42 | 16.63 | 99.33 | | | | | |
| Sodic | | | | | | | | | | | | | | |
| bcs-vwl-0002-03 | 63.15 | 23.28 | 3.73 | 0.05 | 0.17 | 0.04 | 9.08 | 0.54 | 100.03 | | | | | |
| ghn-nwd-0021-21 | 67.62 | 20.23 | 0.19 | 0.03 | 0.04 | 0.01 | 11.51 | 0.22 | 99.85 | | | | | |
| CLAY | P2O5 | SiO2 | SO2 | TiO2 | Al2O3 | MgO | CaO | MnO | FeO | Na2O | K2O | F | Cl | Total |
| Chloritic | | | | | | | | | | | | | | |
| ghn-nwd-0008-20 | 0.00 | 30.90 | 0.00 | 0.01 | 16.42 | 15.96 | 0.15 | 1.16 | 16.87 | 0.99 | 0.29 | 0.60 | 0.02 | 83.36 |
| ghn-nwd-0017-13 | 0.02 | 27.76 | 0.06 | 0.00 | 16.26 | 18.21 | 0.11 | 0.64 | 19.08 | 0.00 | 0.00 | 0.35 | 0.01 | 82.50 |
| Illitic | | | | | | | | | | | | | | |
| ghn-nwd-0021-14 | 0.00 | 46.65 | 0.01 | 0.08 | 26.44 | 1.42 | 0.25 | 0.09 | 2.00 | 0.33 | 8.93 | 0.10 | 0.03 | 86.34 |
| ghn-nwd-0021-15 | 0.04 | 47.95 | 0.00 | 0.07 | 25.53 | 1.57 | 0.15 | 0.05 | 2.22 | 0.51 | 9.34 | 0.43 | 0.03 | 87.89 |
| Kaolinitic | | | | | | | | | | | | | | |
| ghn-nwd-0018-30-39 | 0.00 | 43.10 | 0.24 | 0.00 | 31.23 | 1.04 | 0.61 | 0.00 | 1.49 | 0.05 | 0.11 | 0.23 | 0.22 | 78.33 |
| ghn-nwd-0024-30-14* | 0.47 | 45.46 | 0.37 | 0.00 | 33.24 | 1.95 | 1.03 | 0.04 | 4.76 | 0.02 | 0.63 | 0.00 | 0.01 | 88.00 |
| Smectitic | | | | | | | | | | | | | | |
| ghn-nwd-0020-30-13 | 0.00 | 50.48 | 0.07 | 0.01 | 22.17 | 2.10 | 1.27 | 0.02 | 2.58 | 0.07 | 0.34 | 0.25 | 0.15 | 79.50 |
| ghn-nwd-0020-30-14 | 0.00 | 54.10 | 0.06 | 0.05 | 23.79 | 2.09 | 1.42 | 0.08 | 4.09 | 0.87 | 0.18 | 0.42 | 0.16 | 87.31 |
| Pyrite | S | Fe | Cu | Total | | | | | | | | | | |
| ghn-vwl-0003-20 | 53.30 | 46.35 | 0.02 | 99.67 | | | | | | | | | | |
| ghn-vwl-0003-21 | 53.24 | 46.28 | 0.00 | 99.52 | | | | | | | | | | |
| Calcite | Si(CO3)2 | Al2(CO3)3 | Mg(CO3) | Ca(CO3) | Mn(CO3) | Fe(CO3) | Sr(CO3) | Ba(CO3) | Total | | | | | |
| ghn-nwd-0006-10 | 0.52 | 0.03 | 0.13 | 99.52 | 0.10 | 0.34 | 0.14 | 0.04 | 100.82 | | | | | |
| ghn-nwd-0002-11 | 0.16 | 0.00 | 0.00 | 97.74 | 1.77 | 0.38 | 0.00 | 0.04 | 100.10 | | | | | |
| ghn-vwl-0003-18 | 0.00 | 0.01 | 0.03 | 85.11 | 12.14 | 0.53 | 0.70 | 0.00 | 98.52 | | | | | |
| Epidote | SiO2 | TiO2 | Al2O3 | Cr2O3 | MgO | CaO | MnO | FeO | Na2O | Total | | | | |
| ghn-nwd-0006-08 | 37.01 | 0.00 | 20.92 | 0.00 | 0.05 | 22.95 | 0.11 | 15.83 | 0.01 | 96.88 | | | | |
| ghn-nwd-0017-25 | 37.60 | 0.00 | 23.99 | 0.02 | 0.09 | 23.05 | 0.23 | 12.50 | 0.00 | 97.49 | | | | |
| Fe-oxide | P2O5 | SiO2 | TiO2 | Al2O3 | Cr2O3 | Fe2O3 | MgO | CaO | MnO | NiO | SO2 | Total | | |
| ghn-kmd-0048-31-34 | | 0.06 | 5.39 | 0.45 | 0.15 | 90.11 | 1.99 | 0.05 | 0.23 | 0.03 | | 98.46 | | |
| ghn-kmd-0051-31-36 | | 0.14 | 2.35 | 0.13 | 0.00 | 96.63 | 0.05 | 0.01 | 0.00 | 0.00 | | 99.31 | | |
| ghn-kmd-0056-32-17 | | 2.56 | 0.00 | 0.06 | 0.03 | 90.49 | 0.02 | 0.03 | 0.00 | 0.03 | | 93.21 | | |
| SSW-AAF-0001-30-13 | 7.71 | 4.68 | 0.36 | 5.75 | | 68.62 | 0.02 | 0.17 | 0.00 | | 4.89 | 92.20 | | |
| SSW-AAF-0001-30-22 | 5.65 | 5.88 | 0.98 | 7.65 | | 64.35 | 0.06 | 0.05 | 0.72 | | 2.60 | 87.94 | | |
| SSW-AAF-0001-30-23 | 6.09 | 2.66 | 0.34 | 10.80 | | 70.36 | 0.08 | 0.08 | 0.15 | | 1.91 | 92.47 | | |
| SSW-AAF-0001-30-50 | 2.92 | 7.33 | 0.02 | 3.42 | | 73.98 | 0.13 | 0.08 | 0.02 | | 1.00 | 88.90 | | |
| GHN-JRM-0001-30 | 0.00 | 1.92 | 1.37 | 0.71 | | 88.17 | 0.09 | 0.02 | 0.04 | | | 92.32 | | |
| SSS-VTM-0600-30a | 0.21 | 3.92 | 0.03 | 1.57 | | 78.19 | 0.00 | 0.03 | 0.05 | | | 83.98 | | |
| SSS-VTM-0600-30b | 4.38 | 6.07 | 0.02 | 3.04 | | 79.94 | 0.05 | 0.21 | 0.03 | | | 93.73 | | |
| SSS-VTM-0601-30b | 0.21 | 3.76 | 0.00 | 0.25 | | 85.10 | 0.11 | 0.09 | 0.02 | | | 89.53 | | |
| SSW-AAF-0001-30a | 2.79 | 2.83 | 0.04 | 1.25 | | 80.16 | 0.04 | 0.05 | 0.04 | | | 87.20 | | |
| Gypsum | SO2 | CaO | SrO | BaO | H2O | Total | | | | | | | | |
| ghn-kmd-0071-30-12 | 42.70 | 39.53 | 0.04 | 0.05 | 18.37 | 100.69 | | | | | | | | |
| ghn-kmd-0056-30-04 | 44.43 | 38.71 | 0.00 | 0.03 | 18.71 | 101.88 | | | | | | | | |
| Jarosite | P2O5 | SiO2 | Al2O3 | TiO2 | Fe2O3 | CaO | MgO | MnO | Na2O | K2O | SO3 | Total | | |
| GHN-JRM-0001-30 | 0.46 | 1.19 | 0.79 | 0 | 44.47 | 0.01 | 0.03 | 0.05 | 0.3 | 5.12 | 25.63 | 78.04 | | |
| PIT-VWL-0001-31 | 0.45 | 0.19 | 0.15 | 0.01 | 46.89 | 0 | -0.02 | 0 | 0.2 | 4.36 | 27.80 | 80.03 | | |
| MID-AAF-0003-30 | 0.44 | 2.88 | 1.49 | 0.05 | 37.48 | 0.04 | 0.06 | 0.01 | 0.58 | 4.55 | 20.51 | 68.10 | | |
| SSW-AAF-0001-30 | 2.2 | 0.01 | 0.45 | 0.01 | 49.87 | 0.17 | 0 | 0.01 | 2.3 | 2.72 | 24.95 | 82.69 | | |

Analytical totals of less than 100% for a group of minerals indicate the presence of an unanalysed component, usually H2O, in the mineral phase. Porosity in mineral phases will also reduce analytical totals

APPENDIX 2. Figures.

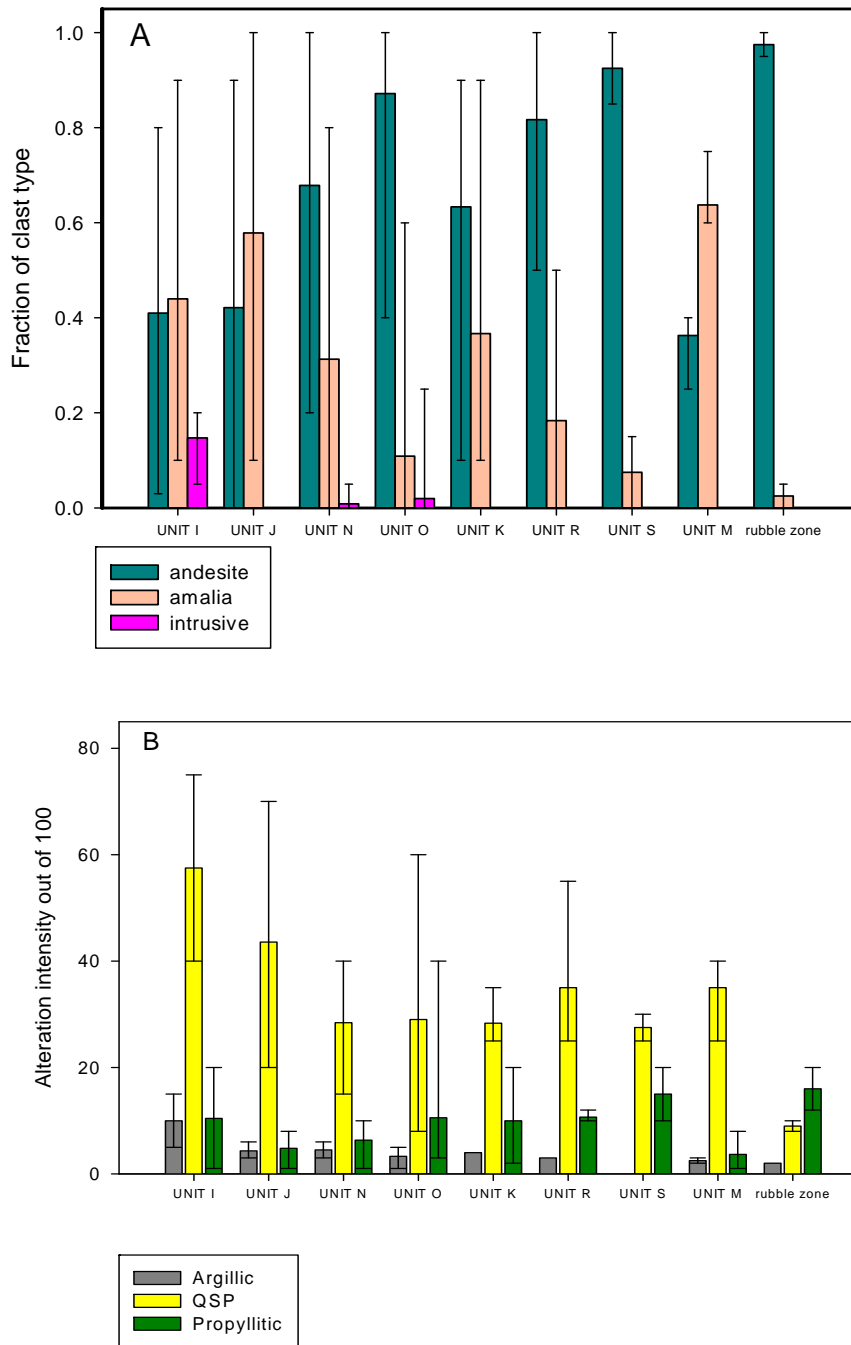


FIGURE 1. Variations of a) lithology and b) alteration intensity by type for geologic units in the rock pile. Averages (colored bars) and range (line) shown.

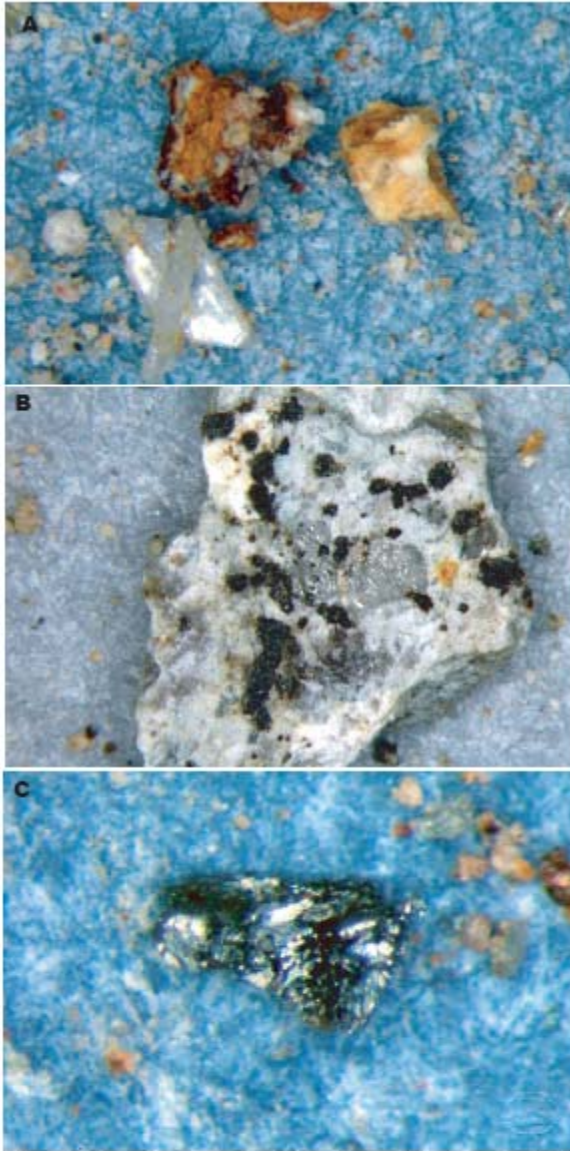


Figure 2. Samples examined for petrographic characterization.
A) Authigenic gypsum, stained detrital gypsum and hematite from GHN-KMD-0081.
B) QSP altered lithic fragment with goethite after pyrite on the surface from GHN-VTM-0216.
C) Oxidized pyrite from GHN-VTM-0420.

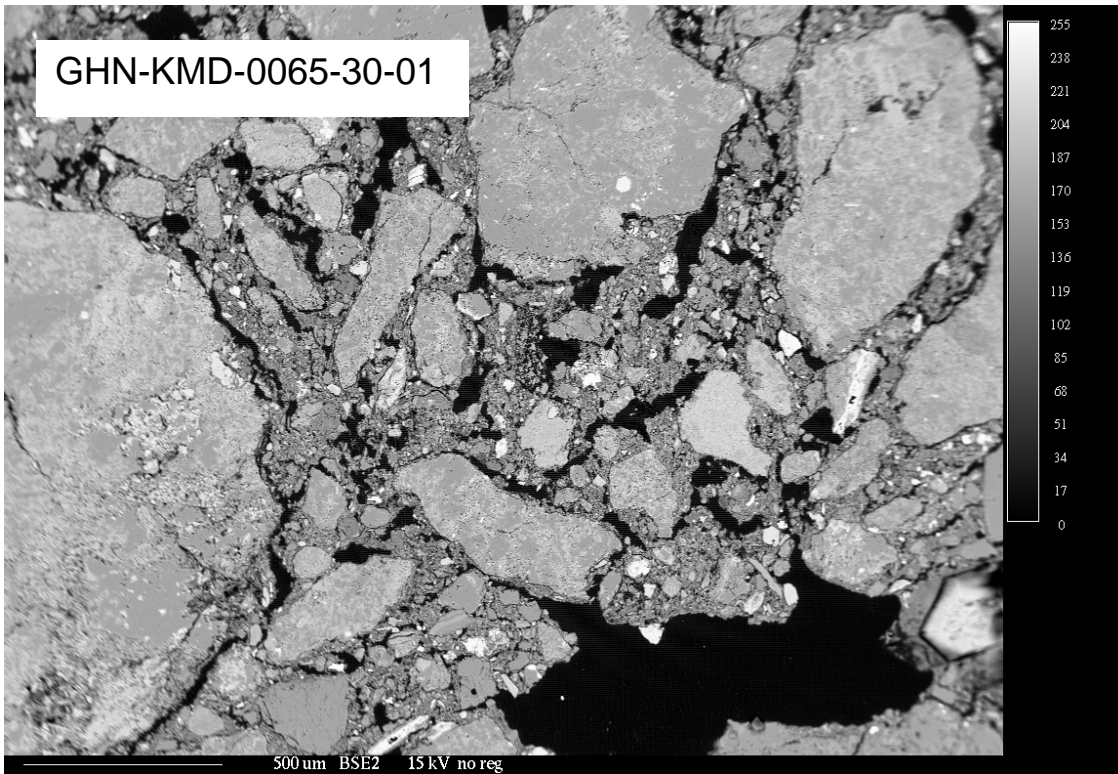


FIGURE 3. Backscattered electron image (BSE) showing soil sample showing rock fragment and associated fine-grained matrix material.

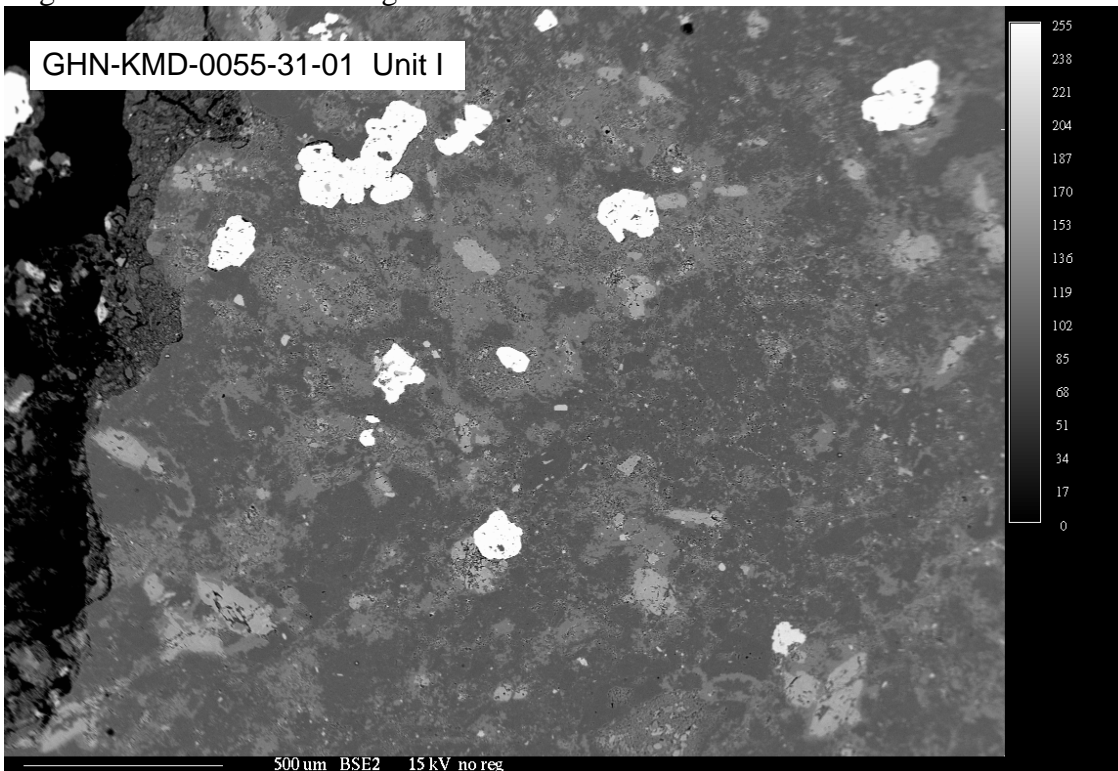


FIGURE 4. BSE image of fresh pyrite in rock sample. Brightest areas on image are pyrite grains, which are of uniform brightness and display distinct grain margins.

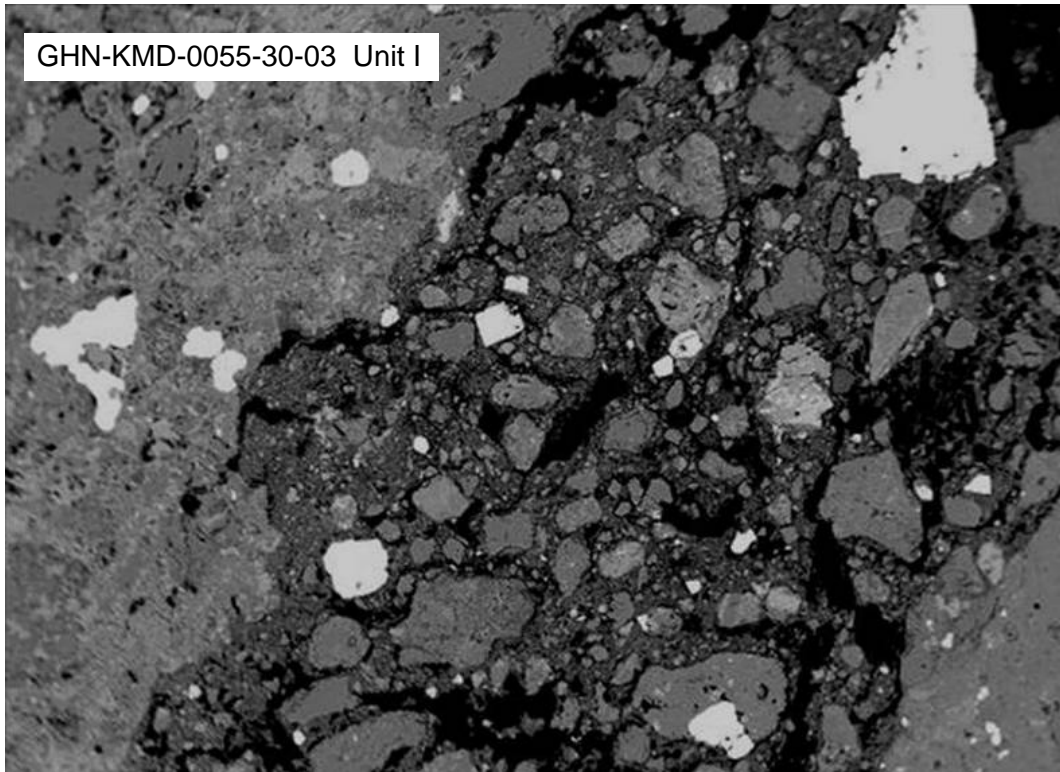


FIGURE 5. BSE image of fresh pyrite in soil sample. Brightest areas on image are pyrite grains, which are of uniform brightness and display distinct grain margins (Field of view = 2.5 mm)

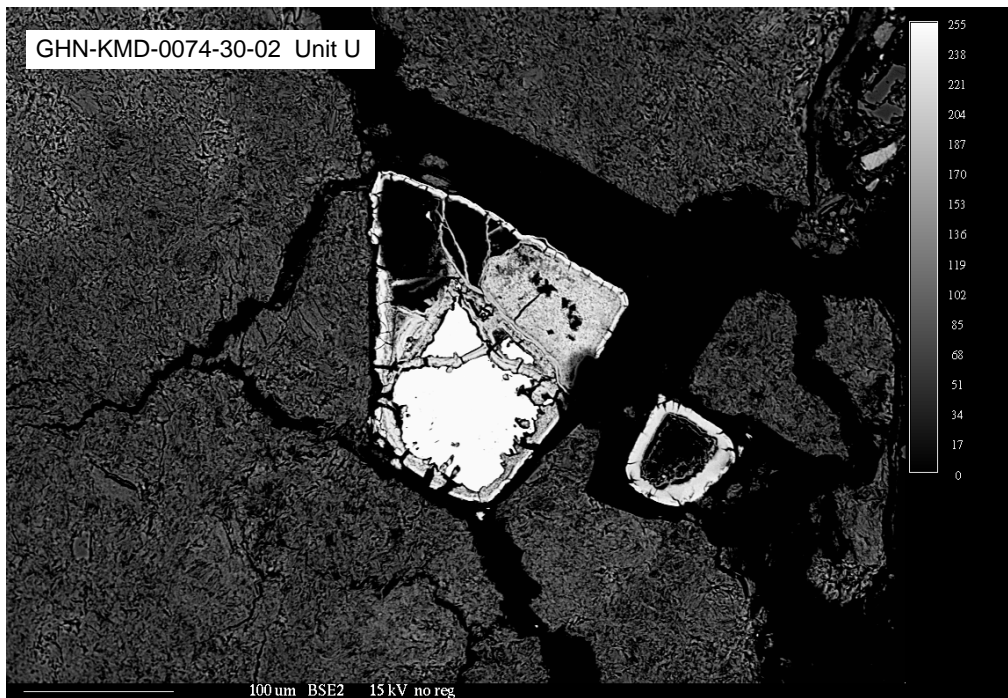


FIGURE 6. Backscattered electron image of residual pyrite core with oxidized rim. Brightest area of image is pyrite, and slightly darker surrounding area is oxidized pyrite.

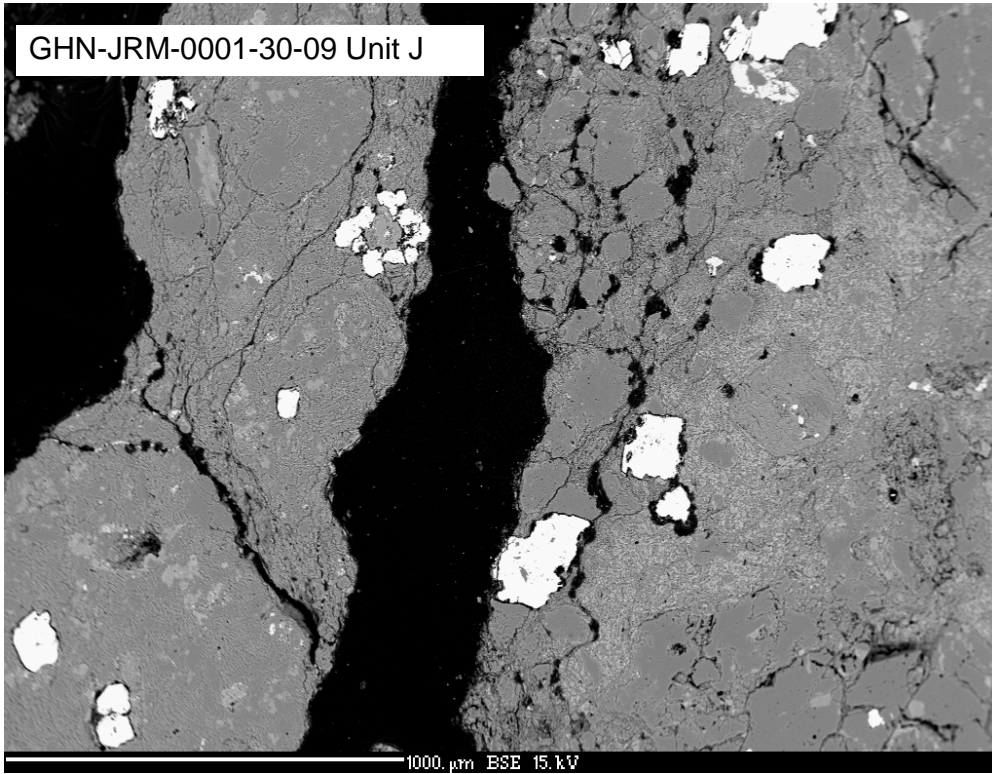


FIGURE 7. BSE image of pyrite grains. Pyrite is brightest areas of image. Dark rims around pyrite are void spaces.

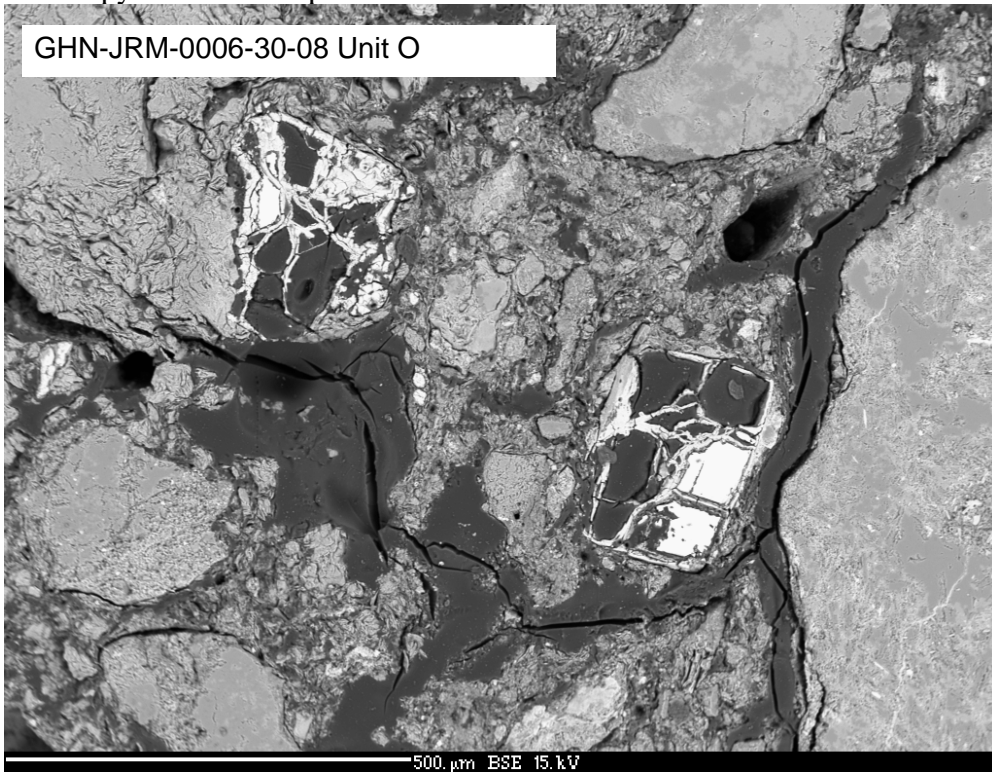


FIGURE 8. BSE image of altered pyrite grain. Brightest area is residual pyrite, but the outline of the original grain, outlined in an oxidized pyrite skeleton, is visible.

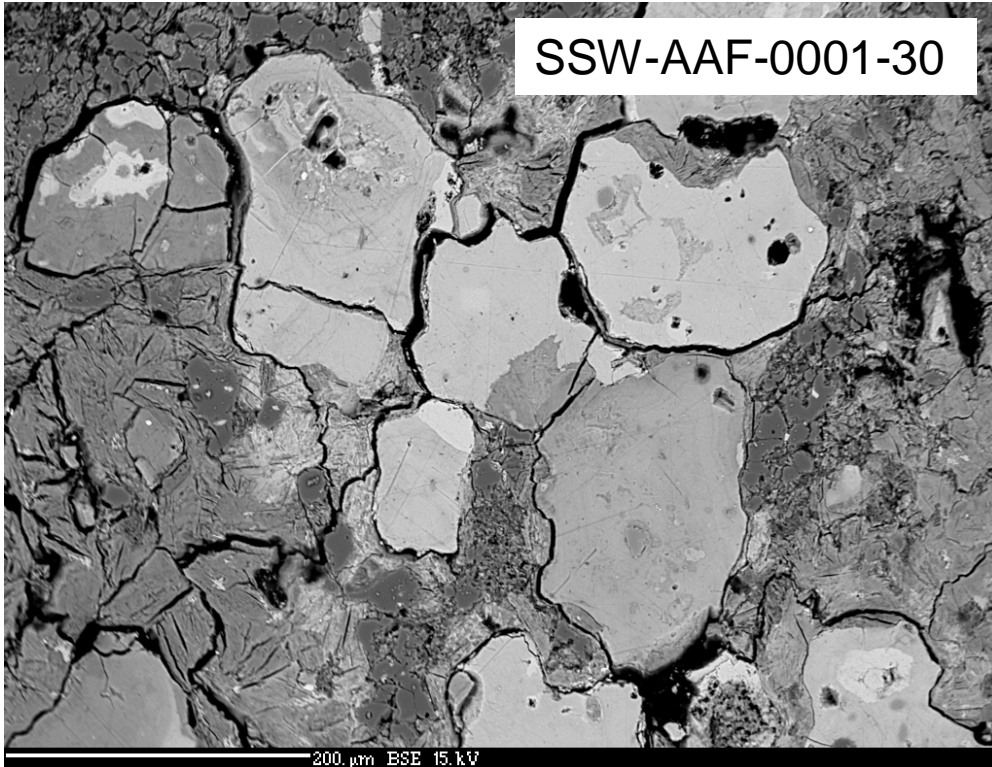


FIGURE 9. Goethite grains that appear to have replaced pyrite

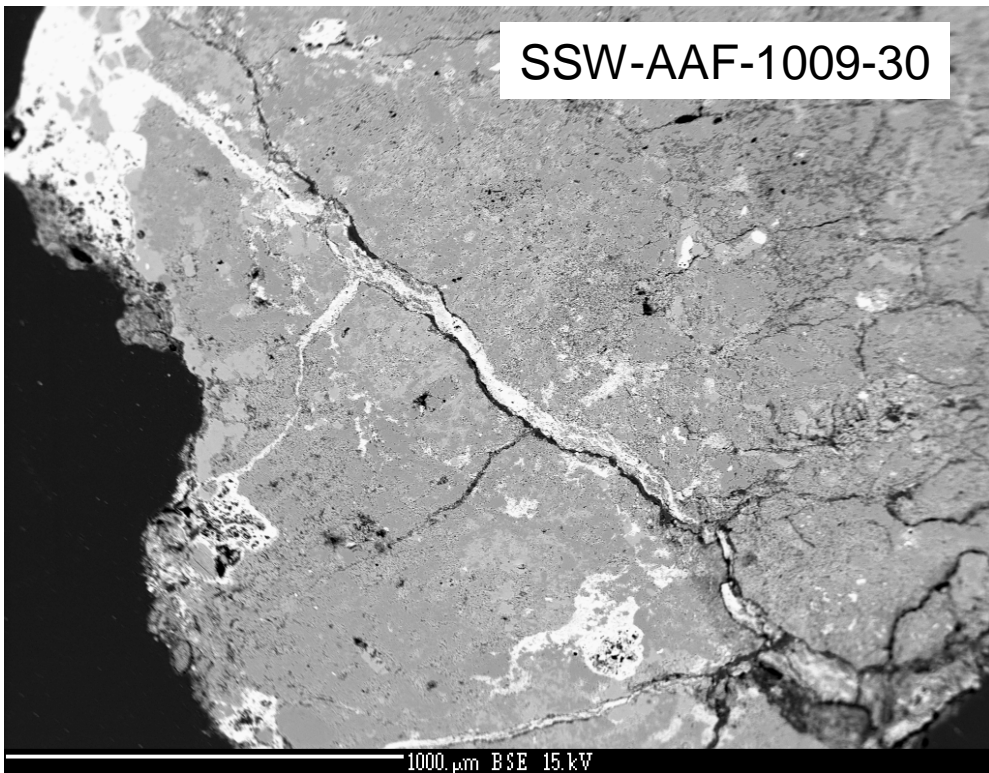


FIGURE 10. Goethite (bright areas) filling a fracture.

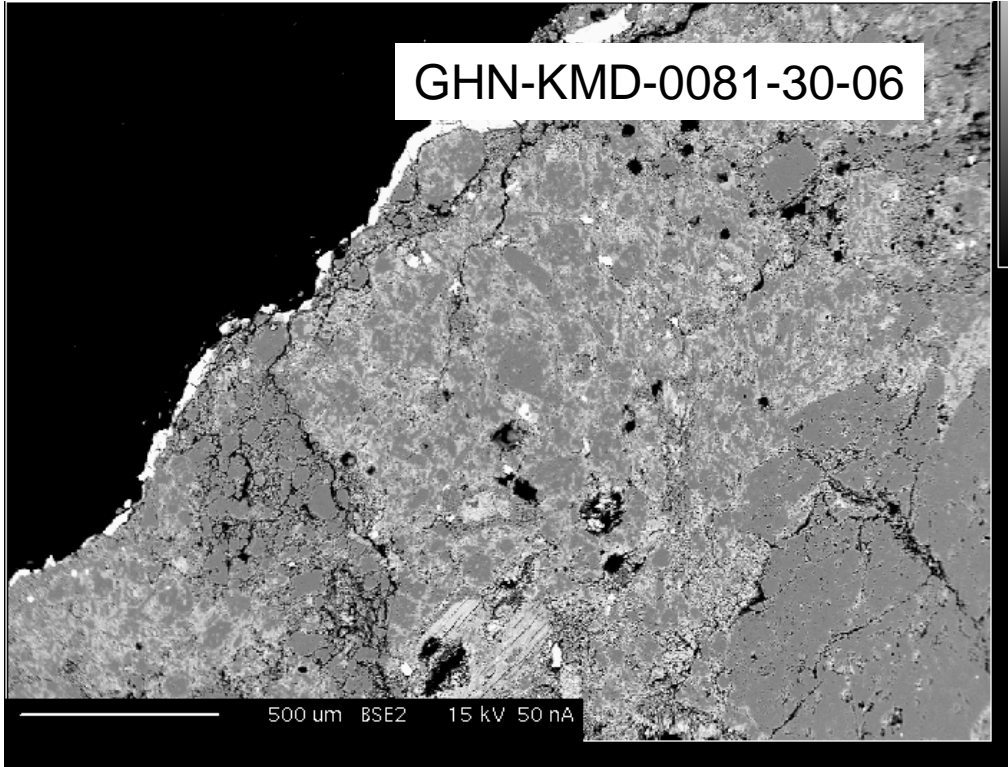


FIGURE 11. Goethite (bright areas) along the edge of a rock fragment.

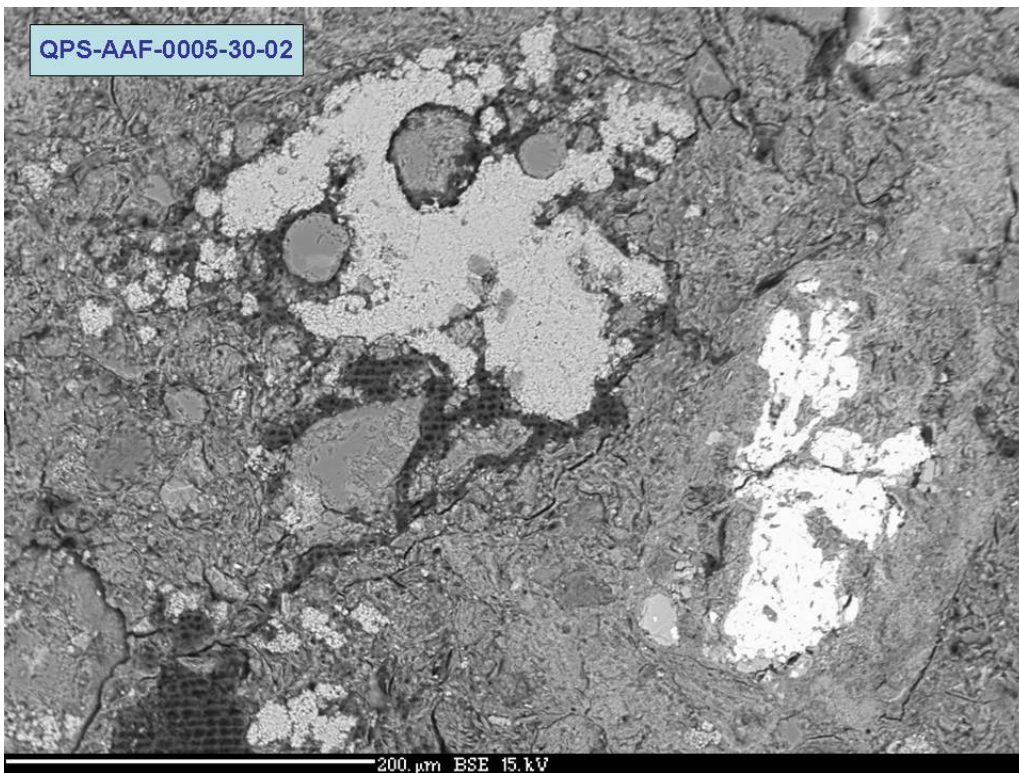


FIGURE 12. BSE image of granular jarosite and P-bearing goethite (bright grain) in soil matrix.

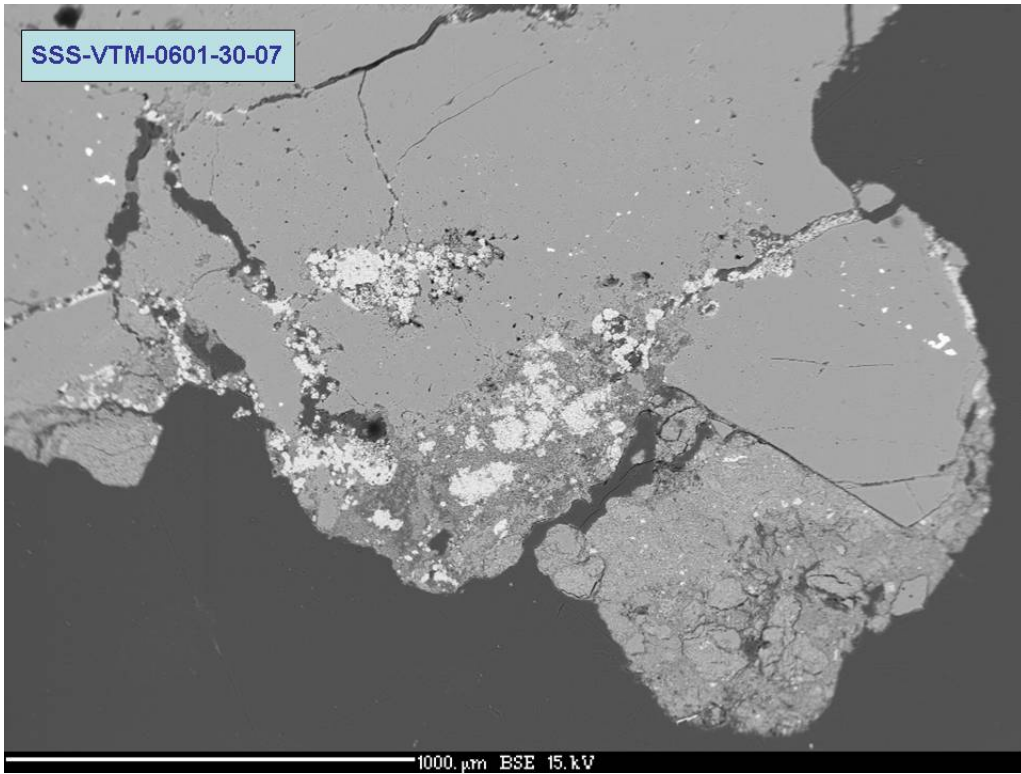


FIGURE 13. BSE image of jarosite aggregate intergrown in soil matrix and filling fractures in altered rock.

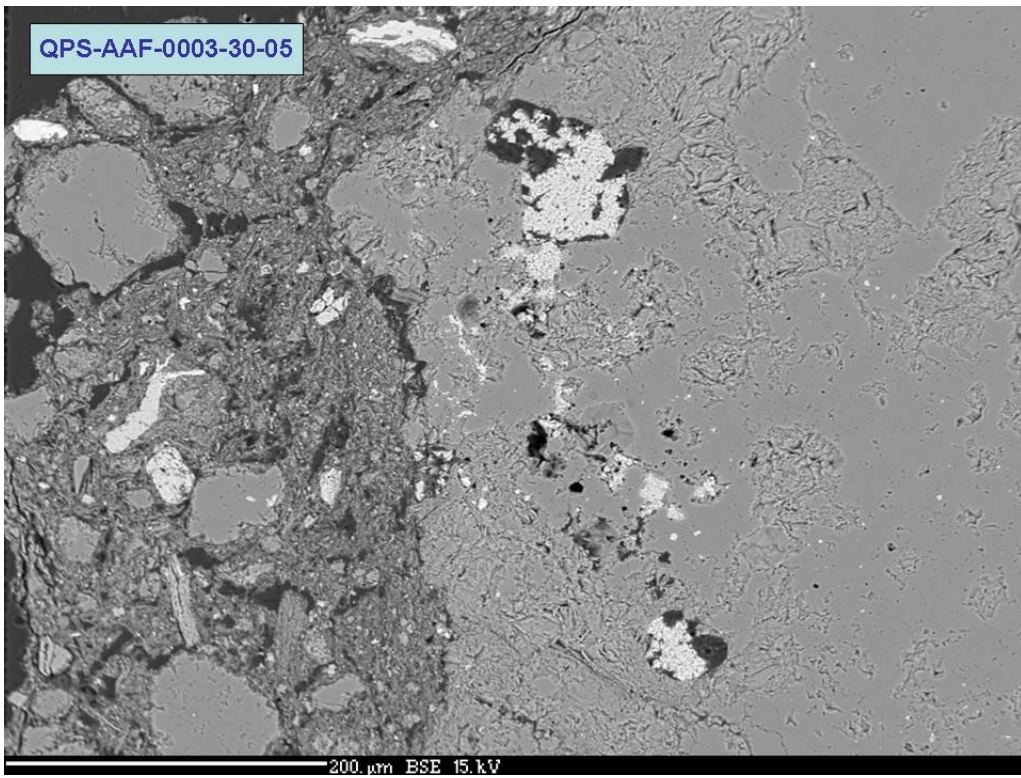


FIGURE 14. BSE image showing partial replacement of relict pyrite cubes by jarosite.

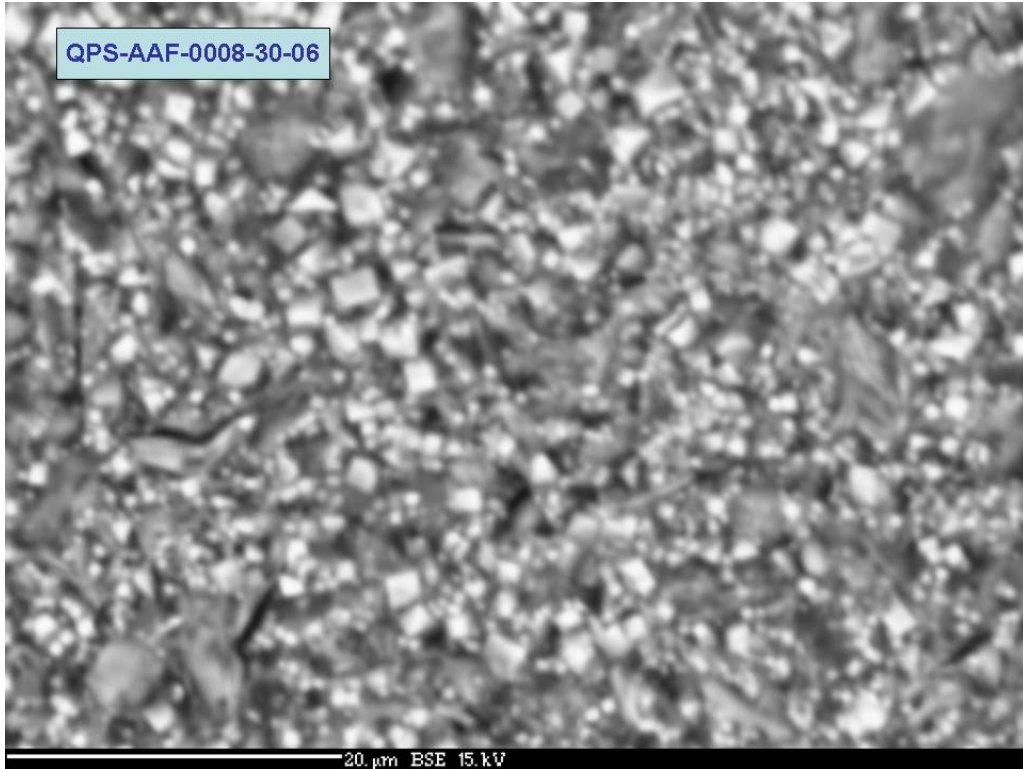


FIGURE 15. BSE image of tiny euhedral jarosite crystals intergrown in soil matrix

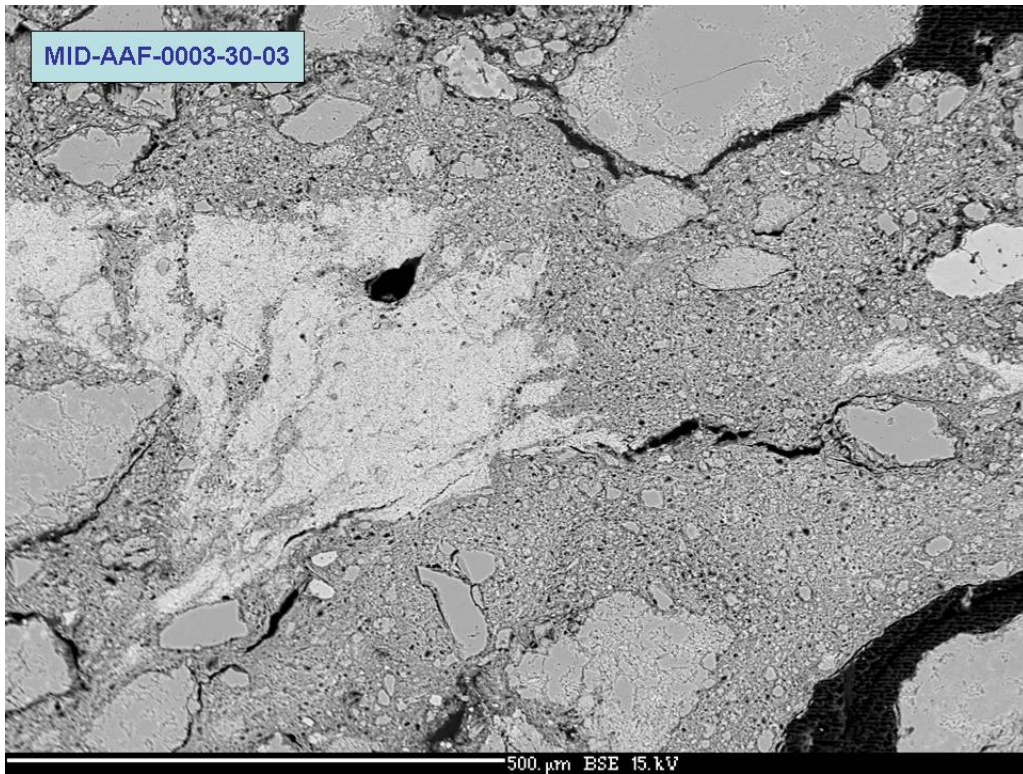


FIGURE 16. BSE image of jarosite cement within finely intermixed jarosite/clay soil matrix.

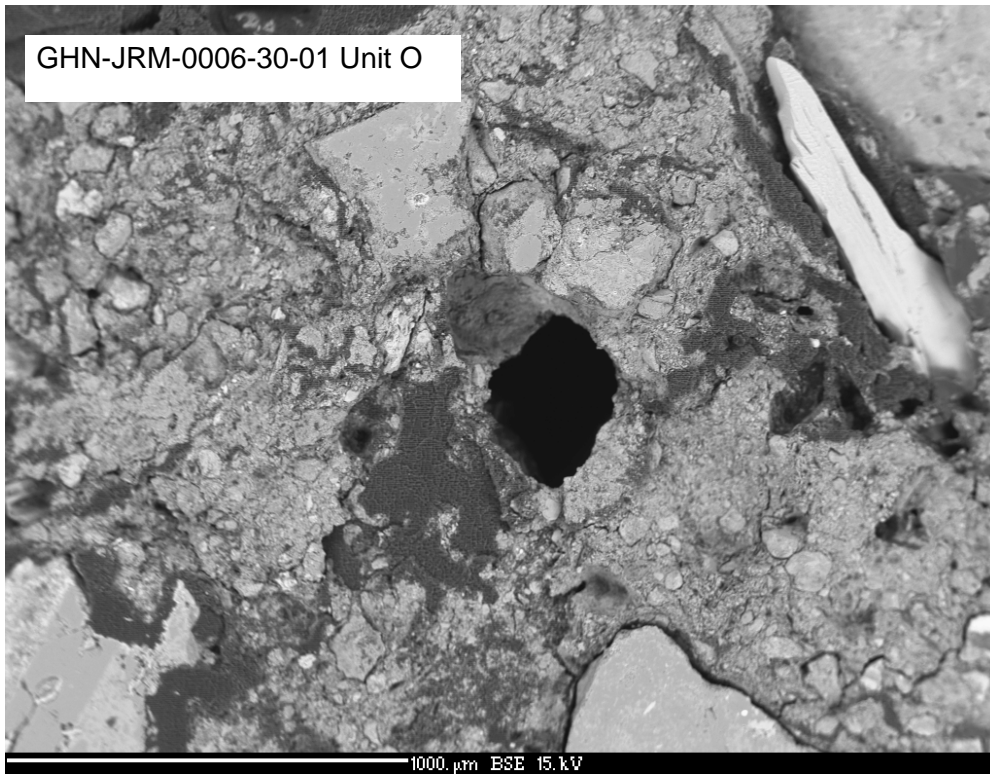


FIGURE 17. BSE image of detrital gypsum. Gypsum is the bright grain in the upper right corner of image.



FIGURE 18. BSE image of gypsum rosettes at the margin of a clot of soil.

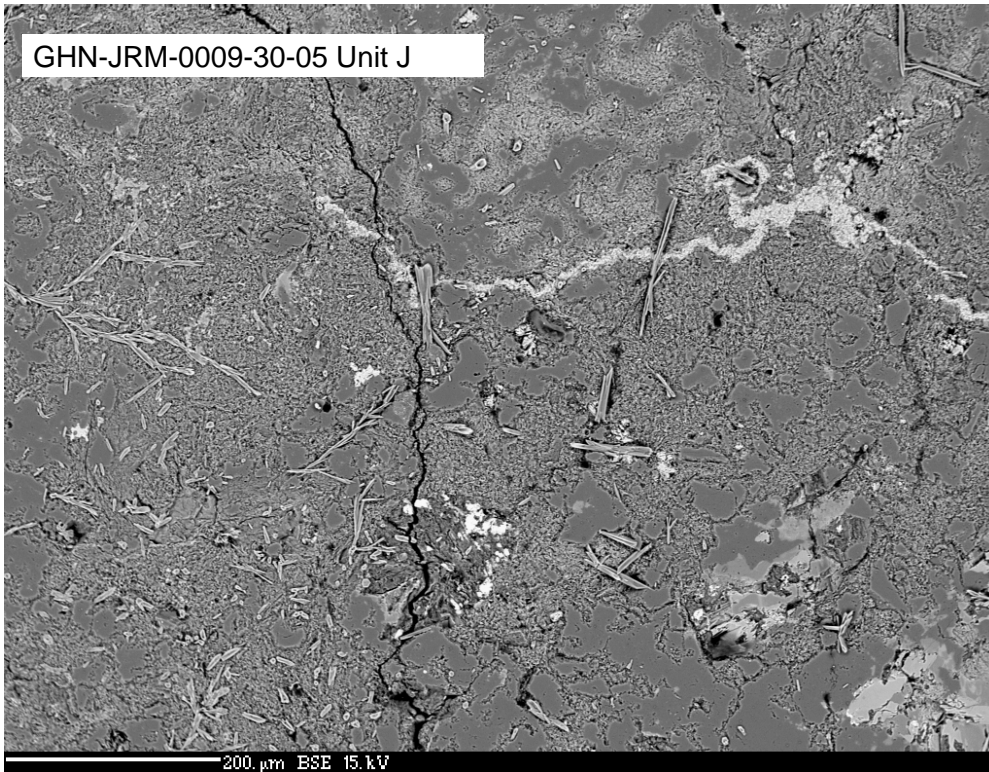


FIGURE 19. BSE image of gypsum needles intergrown in matrix of altered rock fragment in soil sample. The bright, thread-like vein in the upper part of the image is jarosite.